THE JOURNAL OF BIOLOGICAL CHEMISTRY VOL. 286, NO. 20, pp. 18170–18180, May 20, 2011

Phosphatidylethanolamines Modified by γ-Ketoaldehyde (γKA) Induce Endoplasmic Reticulum Stress and Endothelial Activation*

Received for publication, December 16, 2010, and in revised form, March 23, 2011 Published, JBC Papers in Press, March 25, 2011, DOI 10.1074/jbc.M110.213470

Lilu Guo[‡1], Zhongyi Chen[‡1], Brian E. Cox[‡], Venkataraman Amarnath[§], Raquel F. Epand[¶], Richard M. Epand[¶], and Sean S. Davies[‡‖2]

From the [‡]Division of Clinical Pharmacology and Departments of [§]Pathology and [‖]Pharmacology, Vanderbilt University, Nashville, Tennessee 37232-6602 and the [¶]Department of Biochemistry and Biomedical Services, McMaster University, Hamilton, Ontario L8N 3Z5, Canada

Peroxidation of plasma lipoproteins has been implicated in the endothelial cell activation and monocyte adhesion that initiate atherosclerosis, but the exact mechanisms underlying this activation remain unclear. Lipid peroxidation generates lipid aldehydes, including the γ-ketoaldehydes (γKA), also termed isoketals or isolevuglandins, that readily modify the amine headgroup of phosphatidylethanolamine (PE). We hypothesized that aldehyde modification of PE could mediate some of the proinflammatory effects of lipid peroxidation. We found that PE modified by γKA (γKA-PE) induced THP-1 monocyte adhesion to human umbilical cord endothelial cells. γKA-PE also induced expression of adhesion molecules and increased MCP-1 and IL-8 mRNA in human umbilical cord endothelial cells. To determine the structural requirements for γKA-PE activity, we tested several related compounds. PE modified by 4-oxo-pentanal induced THP-1 adhesion, but *N*-glutaroyl-PE and $C_{18:0}$*N*-acyl-PE did not, suggesting that an *N*-pyrrole moiety was essential for cellular activity. As the *N*-pyrrole headgroup might distort the membrane, we tested the effect of the pyrrole-PEs on membrane parameters. γKA-PE and 4-oxo-pentanal significantly reduced the temperature for the liquid crystalline to hexagonal phase transition in artificial bilayers, suggesting that these pyrrole-PE markedly altered membrane curvature. Additionally, fluorescently labeled γKA-PE rapidly internalized to the endoplasmic reticulum (ER); γKA-PE induced C/EBP homologous protein CHOP and BiP expression and p38 MAPK activity, and inhibitors of ER stress reduced γKA-PE-induced C/EBP homologous protein CHOP and BiP expression as well as EC activation, consistent with γKA-PE inducing ER stress responses that have been previously linked to inflammatory chemokine expression. Thus, γKA-PE is a potential mediator of the inflammation induced by lipid peroxidation.

Lipid peroxidation has been implicated in a host of pathological processes, including inflammation and atherosclerosis, but there is still much that is unknown about the mechanisms linking lipid peroxidation to the activation of inflammatory responses. Lipid peroxidation produces a plethora of lipid aldehydes (Fig. 1), including malondialdehyde, acrolein, and 4-hydroxynonenal (HNE).[3] It also produces a large family of γ-ketoaldehydes (γKA), regioisomers that have been given the trivial name of isoketals or isolevuglandins. Exposure of vascular cells to various aldehydes results in endothelial dysfunction, secretion of cytokines, and recruitment of monocytes (1–7), all of which are key steps in the initiation of the chronic inflammatory conditions leading to atherosclerosis.

Despite these potentially important inflammatory effects, the mechanisms whereby lipid aldehydes induce their effects on vascular cells are still poorly understood. Significant effort has focused on the effects of protein and DNA modification by lipid aldehydes. However, recent studies have shown that lipid aldehydes, including malondialdehyde, acrolein, HNE, and γKA, also modify phosphatidylethanolamine (PE) *in vitro* (8–18) as does an aldehyde oxidation product of cholesterol (19). Of particular interest in this regard is our recent finding that treatment of human umbilical vein endothelial cells (HUVEC) with 15-E_2-isoketal, one of the major γKA regioisomers, generated more modified PE (γKA-PE) than modified protein (17). Aldehyde-modified PEs, including γKA-PE, are formed in significant amounts in biological systems during oxidative stress. For instance, *N*-pyrrole-modified PEs (which could arise from reaction of a number of different lipid aldehydes with PE, including γKA) were detected by Ehrlich assay in HDL oxidized *in vitro* (20). Treatment with arachidonic acid, which induces oxidative stress and lipid peroxidation, significantly elevates levels of

* This work was supported, in whole or in part, by National Institutes of Health Grants OD003137-01 (to S. S. D.) and UL1 RR024975 (to Vanderbilt Institute for Clinical and Translation Research). This work was also supported by Vanderbilt Department of Pharmacology (to S. S. D.) and Heart and Stroke Foundation of Ontario Grant T6915 (to R. M. E.).

[1] Both authors contributed equally to this work.

[2] To whom correspondence should be addressed: 2222 Pierce Ave., 506A RRB, Nashville, TN 37232-6602. E-mail: sean.davies@vanderbilt.edu.

[3] The abbreviations used are: HNE, 4-hydroxynonenal; γKA, γ-ketoaldehyde regiosomer 15-E_2-isoketal; PE, phosphatidylethanolamine; NAPE, *N*-acyl-PE; γKA-PE, PE modified by γKA; OPA-PE, PE modified by 4-oxo-pentanal; DiPoPE, dipalmitoleoylphosphatidylethanolamine; OPA, 4-oxo-pentanal; DiPoPE, 1,2-dipalmitoleoyl-*sn*-glycero-3-phosphoethanolamine; DPPE, 1,2-dipalmitoyl-*sn*-glycero-3-phosphoethanolamine; LPE, 1-palmitoyl-2-hydroxy-*sn*-glycero-3-phosphoethanolamine; *N*-glutaryl-PE, glt-PE, 1,2-dipalmitoyl-*sn*-glycero-3-phosphoethanolamine-*N*-(glutaryl); NBD-PE, 1-palmitoyl-2-{12-[(7-nitro-2–1,3-benzoxadiazol-4-yl)amino]lauroyl}-*sn*-glycero-3-phosphoethanolamine; Etn, ethanolamine; oxPCs, oxidized phosphatidylcholines; HUVEC, human umbilical cord endothelial cell; T_H, hexagonal phase transition; ER, endoplasmic reticulum; ROS, reactive oxygen species; TUDCA, tauroursodeoxycholic acid; AEBSF, 4-(2-aminoethyl)-benzenesulfonyl fluoride; HBSS, Hanks' buffered saline solution; ANOVA, analysis of variance; HSA, human serum albumin; CHOP, C/EBP homologous protein CHOP.

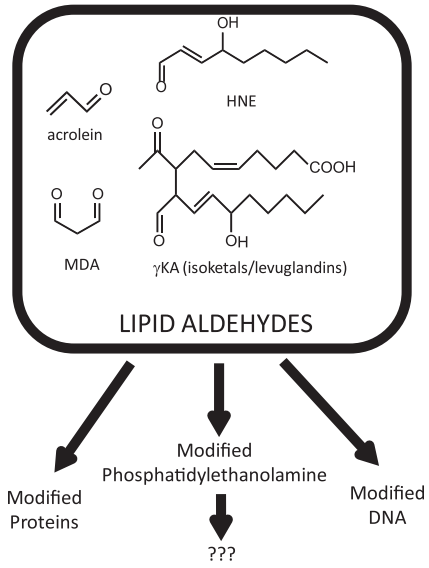

FIGURE 1. **Formation of reactive lipid aldehydes leads to the modification of proteins, DNA, and phosphatidylethanolamine.** Our studies examined the consequences of phosphatidylethanolamine modification. *MDA*, malondialdehyde.

γKA-PE in cultured endothelial cells (21). Chronic ethanol exposure, a well characterized inducer of lipid peroxidation *in vivo*, significantly increases plasma levels of γKA-PEs (18). Plasma levels of γKA-PE are also increased in macular degeneration (18). Although these studies indicate that the lipid aldehydes do indeed modify PE *in vivo*, they do not provide any insight as to whether modification of PE contributes to the proinflammatory activities of lipid aldehydes.

We therefore examined whether γKA-PE could induce proinflammatory effects using a cell culture model of inflammation, THP-1 monocyte adhesion to HUVEC. We then examined the structural requirements for HUVEC activation by γKA-PE and related aldehyde-modified PEs and their effects on membrane bilayer properties. We also assessed the localization of γKA-PE and examined potential mechanisms of cell signaling. These studies suggest that γKA-PE and related pyrrole-PEs are an important new class of proinflammatory mediators that induce their effects through localization to the ER, alteration of membrane curvature, and activation of ER stress signaling pathways.

EXPERIMENTAL PROCEDURES

Reagents—1,2-Dipalmitoleoyl-*sn*-glycero-3-phosphoethanolamine (DiPoPE), 1,2-dipalmitoyl-*sn*-glycero-3-phosphoethanolamine (DPPE), 1-palmitoyl-2-hydroxy-*sn*-glycero-3-phosphoethanolamine (LPE), 1,2-dipalmitoyl-*sn*-glycero-3-phosphoethanolamine-*N*-(glutaryl) (C16:0 glutaryl-PE (glt-PE)), and 1-palmitoyl-2-{12-[(7-nitro-2-1,3-benzoxadiazol-4-yl)amino]lauroyl}-*sn*-glycero-3-phosphoethanolamine (NBD-PE) were purchased from Avanti Polar Lipids (Alabaster, AL). Ethanolamine (Etn), 2,2′-azino-bis(3-ethylbenzothiazoline-6-sulfonic acid) diammonium salt, and LPS were purchased from Sigma. Organic solvents, including methanol, chloroform, dichloromethane, and acetonitrile, were high performance liquid chromatography grade.

Preparation of Lipid Aldehydes and N-Modified PEs—15-E_2-Isoketal, a representative regioisomer of γKA, was prepared as described previously by organic synthesis (22). The synthesis of γKA-PE and γKA-Etn by reaction of 15-E_2-isoketal with DPPE or Etn, respectively, was performed following our previously described procedures (17, 21). γKA-LPE was prepared in a similar manner as γKA-PE except that LPE was used in place of DPPE. To study γKA-PE on membrane parameters, a large scale reaction mixture (100 ml) was concentrated under N_2 and further purified by HPLC. The mobile phase consisted of solvent A (60:20:20 methanol, acetonitrile, 1 mM ammonium acetate) and solvent B (1 mM ammonium acetate in EtOH). The lipids were chromatographed on a Prevail C18 5u (250 × 4.6-mm) column (Alltech, Deerfield, IL) with a constant flow rate of 1 ml/min. After a 2-min hold at 20% solvent B, the solvent was gradient ramped to 100% B over 10 min, held at 100% B for 8 min, and returned to 20% B over 5 min and then held for 5 min before the next injection. The fractions containing γKA-PE were identified by negative ion LC/MS analysis (*m*/*z* 1006.7) and combined. The concentration of final product was determined by parent scan of *m*/*z* 255 in negative ion LC/MS with $C_{17:0}$*N*-acyl-PE (*m*/*z* 942.7) as the internal standard. $C_{17:0}$*N*-acyl-PE, as well as $C_{18:0}$*N*-acyl-PE (NAPE, *m*/*z* 956.7), were prepared as described previously (21).

γKA-NBD-PE was prepared following the same procedure as γKA-PE except NBD-PE was used instead of PE. Excess NBD-PE was removed after reaction using the same HPLC purification method above except that the final product γKA-NBD-PE was quantified by fluorescence using the starting material as reference. 4-Oxo-pentanal (OPA) was prepared as described previously by organic synthesis (23). OPA-PE was prepared from OPA and DPPE following the same procedure as γKA-PE. The HPLC fractions containing OPA-PE were identified by negative ion LC/MS analysis (*m*/*z* 754) and combined.

Cell Culture—HUVEC obtained from the American Type Culture Collection (Manassas, VA) were cultured in endothelial basal growth medium-2 (Lonza, Basel, Switzerland) supplemented with 2% FBS, 0.4% human FGF-B, 0.1% VEGF, 0.1% recombinant long R insulin-like growth factor-B, 0.1% human epidermal growth factor, 0.1% gentamicin sulfate, 0.04% hydrocortisone, 0.1% ascorbic acid, and 0.1% heparin. Cells from passage 6 were used in this study. THP-1 cells were propagated in RPMI 1640 medium containing 10% FBS, 25 mM HEPES, 100 units/ml penicillin, 100 μg/ml streptomycin, L-glutamine, and 50 μmol/liter β-mercaptoethanol.

Preparation of HUVEC Stimulation Solutions—Stimulation solutions of γKA-PE and its analogs were prepared from stock solutions of each *N*-modified PE by evaporating off the organic solvent to dryness, redissolving the *N*-modified PEs in ethanol, diluting to the appropriate concentration using HBSS or DMEM containing 0.1% human serum albumin (HSA), and then sonicating the solution in a water bath sonicator. The final concentration of ethanol was 0.5% or less in all stimulation solutions. Because γKA reacts with the primary amines and is soluble in 0.5% ethanol without the use of HSA, for adhesion assays comparing the potency of γKA with γKA-PE and its analogs, we omitted 0.1% HSA from experiments where γKA

itself was tested and used HBSS, rather than DMEM, because DMEM contains amino acids.

Cell Adhesion Assay—HUVEC (passage 6) were seeded on 0.1% gelatin-coated 96-well culture plates and cultured to 80–90% confluence. Cells were washed with HBSS three times and incubated with vehicle (negative control), LPS (positive control), or the test compound in HBSS at 37 °C for 4 h. The media were removed, and HUVEC cells were washed with HBSS three times prior to adding 100 μl of calcein-labeled THP-1 cells for 1 h at 37 °C. Calcein-labeled THP-1 cells were prepared by incubation with 4 μg/ml calcein acetoxymethyl ester (Invitrogen) at 37 °C for 30 min; excess label was removed by washing three times, and the THP-1 were resuspended in HBSS at 5×10^6 cell/ml. Nonadherent THP-1 cells were removed from HUVEC by gently washing with PBS twice, and the fluorescence of HUVEC-bound THP-1 cells was measured (494 excitation/520 emission). The extent of treatment-induced adhesion for each well was normalized to increase over basal fluorescence in vehicle-treated wells induced by 10 μg/ml LPS. For each compound, a minimum of three separate experiments with five replicate wells per experiment were performed.

To determine the solubility of γKA-PE and its analogs in stimulation solutions used for cultured cell experiments, we prepared solutions containing 1 μM each of γKA-PE, $C_{18:0}$-*N*-acyl-PE, OPA-PE, and glt-PE in either methanol/chloroform (9:1) or in DMEM containing 0.1% HSA and 0.5% ethanol. The *N*-modified PE in the media were then extracted using 2 volumes of chloroform/methanol (2:1); $C_{17:0}$NAPE was added as internal standard, and the amount of *N*-modified PE was quantified by mass spectrometry. Solubility was calculated as the amount of *N*-modified PE measured in the extract of the DMEM, 0.1% HSA compared with that measured in the methanol/chloroform sample. The solubility of each PE in DMEM, 0.1% HSA was as follows: glt-PE, 118%; $C_{18:0}$NAPE, 107%; OPA-PE, 85%; and γKA-PE, 109%. Therefore, all of the *N*-modified PEs appeared to be highly soluble in stimulation media. To assess the extent that each *N*-modified PE as incorporated by HUVEC, we incubated the mixture containing 1 μM of each *N*-modified PE dissolved in the DMEM, 0.1% HSA, 0.5% ethanol with triplicate wells of HUVEC for 4 h, removed the mixture, washed the cells twice, added $C_{17:0}$NAPE as internal standard, extracted the cellular phospholipids with chloroform/methanol (2:1) solution, and then analyzed by mass spectrometry. Incorporation of each of the *N*-modified PEs was as follows: glt-PE, 28%; $C_{18:0}$NAPE, 33%; OPA-PE, 7%; and γKA-PE, 10%.

Expression of Adhesion Molecules—HUVEC (passage 6) were seeded and treated as described above, except that HUVEC were incubated with serum-free DMEM for 1 h prior to treatment with vehicle, γKA-PE, or LPS in DMEM with 0.1% HSA for 4 h. Cell-based ELISAs were then performed as described previously (24). Briefly, cells were washed with PBS containing 0.1% Tween (pH 7.4) and fixed with 1% paraformaldehyde for 0.5 h at room temperature. Excess paraformaldehyde was quenched by incubation with 1% glycine for 1 h. Primary antibodies against ICAM-1 (sc-18853, Santa Cruz Biotechnology, Santa Cruz, CA), VCAM-1 (sc-8304, Santa Cruz Biotechnology), or E-selectin (sc-14011, Santa Cruz Biotechnology) was added to each well and incubated at 4 °C overnight. The wells were washed; HRP-conjugated anti-mouse IgG antibody (Promega, Madison, WI) was added for 1 h, and the immunocomplexes were quantified by absorbance at 405 nm using 2,2′-azino-bis(3-ethylbenzothiazoline-6-sulfonic acid) diammonium salt as peroxidase substrate. Expression was expressed as fold vehicle-only control.

Chemokine mRNA Expression—Levels of IL-8, MCP-1, and GAPDH mRNAs were measured after conversion to cDNA by quantitative real time PCR using IQ SYBR Green supermix (Bio-Rad). The primer pairs for each gene are listed as follows: (*a*) human IL-8 (NM_000584, from Sigma): sense GAG TGC TAA AGA ACT TAG ATG TCA G, antisense GCT TTA CAA TAA TTT CTG TGT TGG C, and probe TGG TCC ACT CTC AAT CAC TCT CAG T; (*b*) human MCP-1 (NM-002982, CCL2, from Sigma): sense CTC TCG CCT CCA GCA TGA AAG, antisense AGG TGA CTG GGG CAT TGA TTG, and probe CTG CCG CCC TTC TGT GCC TGC TG; and (*c*) human GAPDH (NM_002046 GAPDH, from Sigma): sense CAA AAT CAA GTG GGG CGA TGC, antisense CAA ATG AGC CCC AGC CTT CTC, and probe AGT CCA CTG GCG TCT TCA CCA CCT T. Data from five separated experiments were averaged.

Membrane Curvature and T_H—Shifts in the bilayer to hexagonal phase transition temperature of DiPoPE (T_H) upon addition of a membrane additive is a sensitive indicator of the effect of the additive on membrane curvature (25). Lipid films were made by first dissolving DiPoPE with or without a modified PE in chloroform/methanol, 2:1 (v/v), at the appropriate ratios. The solvents were driven off by a stream of nitrogen, and the samples were kept for 3 h under high vacuum to remove the last traces of solvent. Dry lipid films were suspended in 20 mM PIPES, 1 mM EDTA, 150 mM NaCl (pH 7.4) by vortexing to form multilamellar vesicles. The concentration of lipid in the samples studied was maintained at 2.5 mg/ml. Differential scanning calorimetry measurements were made using a Nano II differential scanning calorimeter (Calorimetry Sciences Corp., Lindon, UT). The cell volume was 340 μl. The scan rate was 1 °C/min with a delay of 5 min between sequential scans in a series to allow for thermal equilibration. The features of the design of this instrument have been described (26). The calorimetry curves were analyzed by using the fitting program, DA-2, provided by Microcal Inc. (Northampton, MA), and plotted with Origin, version 7.0.

Localization of γKA-PE—HUVECs were treated with 1 μM γKA-NBD-PE for 1 h at 4 °C to allow the modified PE to accumulate in the plasma membrane of the cell. After 1 h, the cells were transferred to a humid incubator at 37 °C for 15 min, then washed twice with PBS, and fixed for 15 min with 2.5% paraformaldehyde in PBS at room temperature. After fixation, the cells were rinsed three times with PBS containing 1% BSA and 0.1% saponin for 5 min per wash. The cells were then incubated in a humid chamber in the presence of the mouse anti-calnexin antibody (Cell Signaling Technology, Danvers, MA) overnight at 4 °C. After incubating, the cells were rinsed four times in blocking buffer and then incubated with a goat anti-mouse antibody labeled with Alexa 547 fluorophore (Invitrogen) for 1 h at room temperature. At that point, the antibodies were

fixed in place using 2.5% paraformaldehyde for 15 min at room temperature. Imaging was performed using a Zeiss Axioplan imaging upright microscope (Zeiss, Germany) using MetaMorph as the imaging software (Molecular Devices Inc.)

To determine whether γKA-NBD-PE remained intact or was hydrolyzed during the incubation with HUVEC prior to fluorescence imaging, we incubated γKA-NBD-PE with either cell-free buffer or with HUVEC for 1 h at 4 °C and then for 15 min at 37 °C. After this incubation period, the solution was removed from cells; lipids were extracted using acidic modified Bligh-Dyer to ensure extraction of NBD-fatty acid metabolites, and the products were analyzed by TLC using chloroform, methanol, ethanol, ethyl acetate, 0.25% potassium chloride (10:4:10:10:3.6) as solvent. γKA-NBD-PE and γKA-NBD-PE treated with *Streptomyces chromofuscus* phospholipase D (to produce NBD-phosphatidic acid), and γKA-NBD-PE treated with 0.35 N sodium hydroxide (to produce NBD-fatty acid) were used as references. By this analysis, the majority of NBD label remained as intact γKA-NBD-PE. The identity of the major NBD component as γKA-NBD-PE was verified by mass spectrometry.

Immunoblotting of ER Stress Response Proteins—HUVEC were cultured in 100-mm dishes and treated with 3 μM PE or 3 μM γKA-PE for the designated time. After treatment, cells were washed, scraped, centrifuged, and resuspended in lysis buffer (prepared from 20× lysis buffer stock (C7027, Invitrogen) with complete protease inhibitor mixture (Roche Applied Science), 1 mM sodium orthovanadate, 1 mM sodium fluoride, 1 mM sodium molybdate, and 10 mM β-glycerophosphate added), and incubated on ice for 30 min. Lysates were then centrifuged to remove debris and stored at −20 °C until immunoblot analysis. 20 μl of lysate for each sample were separated by SDS-PAGE and transferred to PVDF membrane, and the membrane was cut into three strips for immunoblotting of appropriate ER stress response proteins as follows: <30 kDa (for CHOP), 34–70 kDa (for phospho-p38), and >70 kDa (for BiP/grp78). Each strip was incubated with appropriate primary antibody for CHOP (L63F7, Cell Signaling Technology), BiP/grp78 (C50B12, Cell Signaling Technology), or phospho-p38 (9211S, Cell Signaling Technology) and then visualized using fluorescent anti-mouse or anti-rabbit IgG antibody and scanned by the Odyssey Imaging System (LI-COR Biosciences). After phospho-p38 immunoblotting, the membrane was stripped using Western blot stripping buffer (Pierce, 21059) and re-immunoblotted using antibody for actin (sc-1616-R, Santa Cruz Biotechnology). Data from five separated experiments was analyzed by blot volume (INT/mm^2) with Quantity One software (Bio-Rad). Actin volume was used for normalization. In two replicate experiments, total p38 (9212, Cell Signaling Technology) at the 60-min time point was also measured by immunoblotting, and the ratio of phospho-p38 to total p38 was determined.

Inhibition of ER Stress Response—Two commonly used ER stress response inhibitors, tauroursodeoxycholic acid (TUDCA) and 4-(2-aminoethyl)benzenesulfonyl fluoride (AEBSF), were used to test the effect of inhibiting ER stress response signaling. Confluent HUVEC were pretreated with either vehicle, 300 μM AEBSF, or 300 μM TUDCA for 1 h, and the pretreatment media were removed and replaced with stimulation buffer containing γKA-PE. For experiments to measure CHOP and BiP expression, 100-mm dishes were used, and lysate preparation and immunoblotting were performed as described above with HUVEC being stimulated with 3 μM γKA-PE for 1 h. For adhesion assays, 96-well plates were used, and HUVEC were stimulated with 2 or 5 μM γKA-PE for 4 h prior to performing the THP-1 adhesion assay as described above.

Statistical Analysis—All statistical analysis was performed using Graph Pad Prism 4.03 (GraphPad Software, La Jolla, CA).

RESULTS

PE Modified by an Endogenous γ-Ketoaldehyde Induces Endothelial Cell Activation—ROS have previously been associated with activation of endothelial cells and inflammation. We hypothesized that formation of γKA-PE (or its metabolites) would be an important mediator of ROS-induced inflammation (Fig. 2*A*). To confirm that ROS induced inflammation, we treated confluent monolayers of HUVEC with 0–1 mM H_2O_2 and then measured the adhesion of calcein-labeled THP-1 monocytes to the stimulated HUVEC by fluorescence. THP-1 adhesion was normalized as the percent of fluorescence induced by 10 μg/ml LPS after subtraction of base-line fluorescence in vehicle-only treated cells. H_2O_2 dose-dependently (EC_{50} 0.13 mM) induced adhesion of THP-1 monocytes to HUVEC (Fig. 2*B*). We then tested if 15-E_2-isoketal, one of the eight regioisomers of γKA that are generated by peroxidation of arachidonic acid and that are the immediate precursors to γKA-PE, could also induce similar effects. We found that γKA also dose-dependently (EC_{50} 3.5 μM) increased THP-1 adhesion to HUVEC (Fig. 2*C*). We have previously shown that the major product formed when γKA is added to HUVEC is γKA-PE, although γKA protein adducts form as well (17). To determine whether the formation of γKA-PE was sufficient to induce HUVEC activation, we synthesized γKA-PE using 15-E_2-isoketal as a representative regioisomer, and we tested its effect on HUVEC. Direct addition of γKA-PE to HUVEC dose-dependently (EC_{50} 2.5 μM) increased THP-1 binding to HUVEC (Fig. 2*D*).

Some *N*-modified PEs (*e.g.* NAPE) require hydrolysis of the parent phospholipid to generate the bioactive compound (*i.e. N*-acylethanolamides). Although the metabolism of γKA-PE in HUVEC has not been studied, purified PLA_2 can hydrolyze γKA-PE *in vitro* to its lyso-PE analog (γKA-LPE) (18), and we have shown that phospholipase D isolated from *S. chromofuscus* can hydrolyze γKA-PE *in vitro* to its ethanolamine analog (γKA-Etn) (17). To test whether these potential metabolites of γKA-PE might be the actual active form of γKA-PE, we synthesized γKA-LPE and γKA-Etn and tested their effects on HUVEC. Although both γKA-LPE and γKA-Etn dose-dependently induced THP-1 adhesion to HUVEC, neither γKA-LPE (EC_{50} 11.1 μM, Fig. 2*E*) nor γKA-Etn (EC_{50} 18.6 μM, Fig. 2*F*) were as potent as γKA-PE itself, suggesting that hydrolysis of γKA-PE was not necessary for its activity.

γKA-PE Induces Expression of Adhesion Molecules and Chemokine Secretion—Attraction and tight adhesion of leukocytes to endothelial cells usually require expression of chemokines such as MCP-1 and IL-8 as well as surface display of adhe-

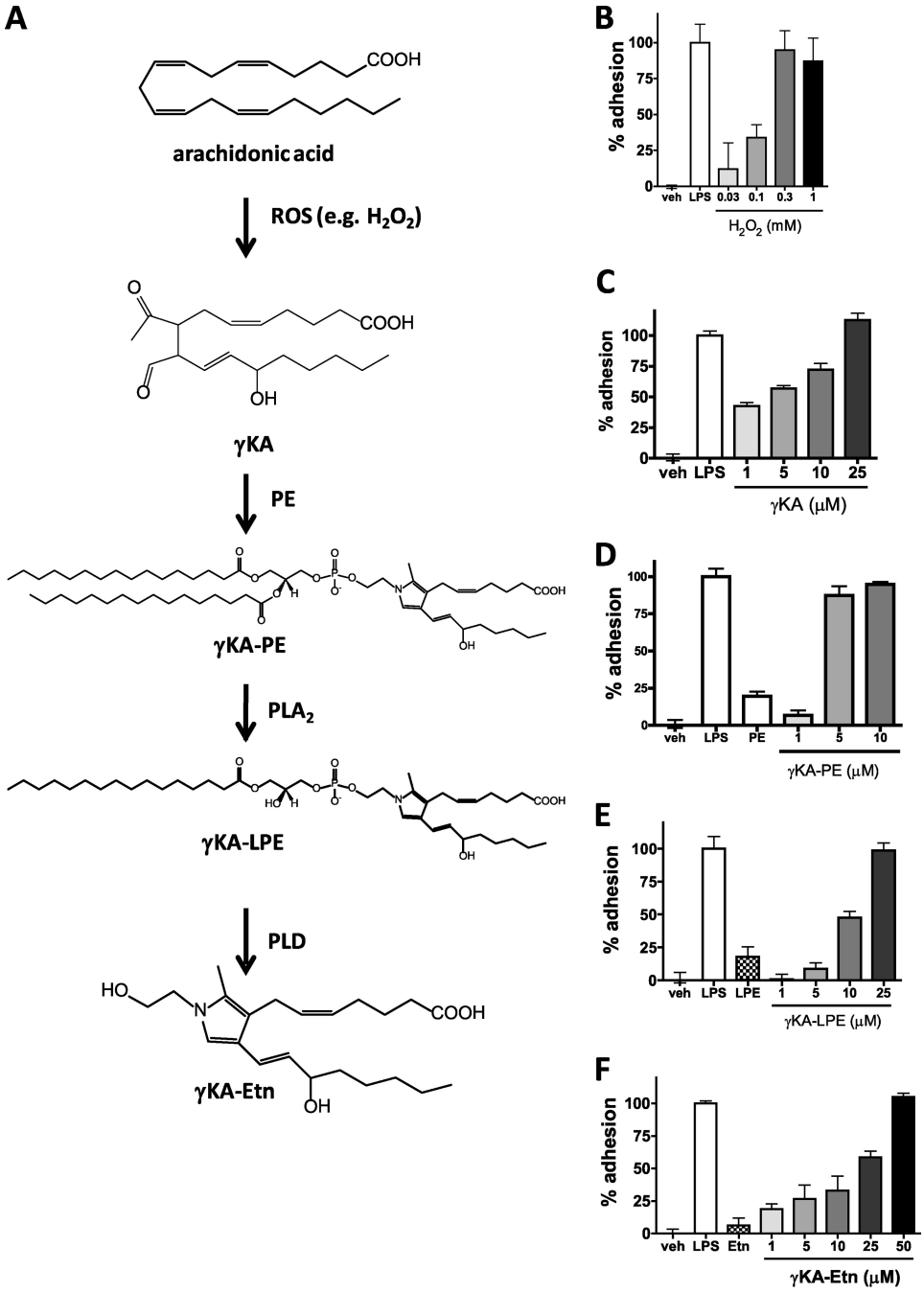

FIGURE 2. **Induction of THP-1 adhesion to HUVEC by precursors and products of the formation of γKA-PE.** HUVEC were treated with varying concentrations of γKA-PE precursors, and activation of HUVEC was measured by adhesion of calcein-labeled THP-1 as described under "Experimental Procedures." *A,* schematic of γKA-PE formation. Peroxidation of arachidonate (either free or esterified to phospholipids) by ROS, including hydrogen peroxide, leads to the formation of many lipid peroxidation products, including a family of γKA regioisomers (represented here by 15-E_2-isoketal). These γKA rapidly modify primary amines present in the membrane, including proteins and PE (γKA-PE). Preparations of phospholipases A_2 (PLA_2) and D (*PLD*) can hydrolyze γKA-PE *in vitro* to form γKA-LPE and γKA-Etn, respectively. *B,* H_2O_2 treatment of HUVEC induces concentration-dependent THP-1 adhesion (one-way ANOVA, $p < 0.0001$). *C,* γKA induces THP-1 adhesion to HUVEC in a concentration-dependent manner (one-way ANOVA, $p < 0.0001$). *D,* γKA-PE induces THP-1 adhesion to HUVEC in a concentration-dependent manner (one-way ANOVA, $p < 0.0001$). *E,* γKA-LPE induces THP-1 adhesion in a concentration-dependent manner, although less potently than γKA-PE (one-way ANOVA, $p < 0.0001$). *F,* γKA-Etn induces THP-1 adhesion in a concentration-dependent manner, although less potently than γKA-PE (one-way ANOVA, $p < 0.0001$). *veh*, vehicle.

sion molecules such as ICAM-1, VCAM-1, and E-selectin. We therefore investigated whether γKA-PE induced expression of these molecules in HUVEC. After treatment of HUVEC with γKA-PE for 4 h, we observed a dose-dependent increase in the expression levels of ICAM-1 (one-way ANOVA, $p < 0.0001$; Fig. 3*A*), VCAM-1 (one-way ANOVA, $p < 0.0001$; Fig. 3*B*), and E-selectin (one-way ANOVA, $p = 0.0149$; Fig. 3*C*). After treatment of HUVEC with γKA-PE, we also detected significant increases by quantitative real time PCR in mRNA levels of both MCP-1 (Fig. 4*A*) and IL-8 (Fig. 4*B*). These observations are consistent with γKA-PE inducing THP-1 monocyte adhesion by standard proinflammatory mechanisms.

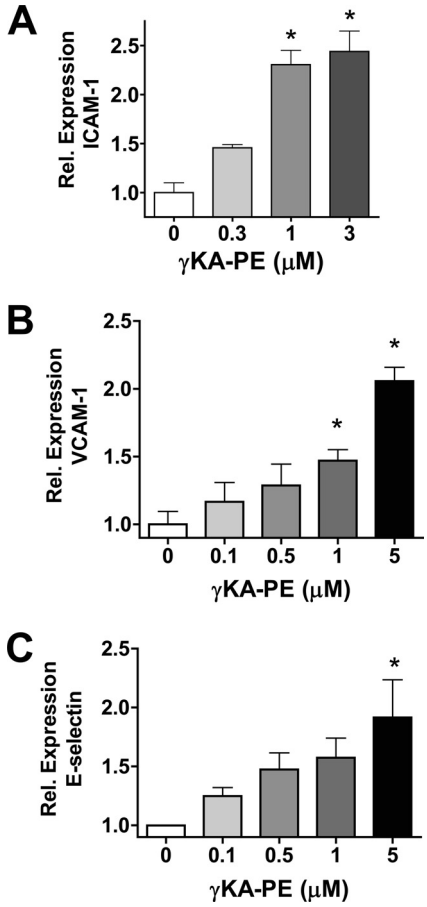

FIGURE 3. **γKA-PE dose-dependently induces expression of adhesion molecules in HUVEC.** *A,* expression of adhesion molecules was measured by cell-based immunoassay after paraformaldehyde fixation of HUVEC as described under "Experimental Procedures." *A,* ICAM-1 (one-way ANOVA, $p < 0.0001$). *B,* VCAM-1 (one-way ANOVA, $p < 0.0001$). *C,* E-selectin (one-way ANOVA, $p = 0.0149$). *, significantly differ from 0 μM γKA-PE by Dunnett's post-test.

Pyrrole Moiety Is the Key Structural Feature for γKA-PE Activity—We next sought to understand the structural components that were required for γKA-PE activity. In particular, we hypothesized that the side chain with the carboxylate anion moiety, which we anticipated would form a "lipid whisker"-like structure, would be important for activity, as lipid whiskers appear to be a key structural determinant of the activity of pro-inflammatory oxidized phosphatidylcholines (oxPCs). We also considered the possibility that the two other structural features of γKA-PE, a large aliphatic headgroup or the pyrrole moiety, might also be required for bioactivity. To determine whether any of these structural features were required for activity, we analyzed a series of γKA-PE analogs for their ability to activate HUVEC (Fig. 5*A*). To test the requirement for a carboxylate acyl chain, we used *N*-glutaroyl-PE. To test the requirement for a large aliphatic headgroup, we used $C_{18:0}$*N*-acyl-PE (NAPE). To test the requirement for a pyrrole headgroup, we reacted OPA with PE and isolated the resulting pyrrole adduct (OPA-PE). We then tested 5 μM of each of these compounds in the THP-1 adhesion assay. OPA-PE induced HUVEC activation to nearly the same extent as LPS and γKA-PE, whereas NAPE and glt-PE failed to induce cell adhesion (Fig. 5*B*). Higher concentrations of NAPE and glt-PE (25 μM) also failed to induce cell adhesion (data not shown.) The failure to induce cell adhesion was not due to lack of incorporation into HUVEC, as glt-PE and NAPE were incorporated to a slightly greater extent than γKA-PE. These results suggested that the pyrrole moiety of γKA-PE was the key structure required for its activity.

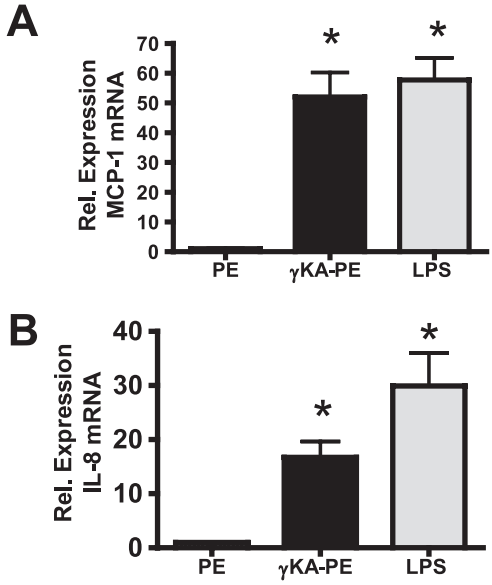

FIGURE 4. **γKA-PE (1 μM) induces increased mRNA expression for inflammatory chemokines in HUVEC.** mRNA for chemokines were measured using quantitative real time PCR with normalization to GAPDH as described under "Experimental Procedures." *A,* γKA-PE induces MCP-1 chemokine expression (*, two-tailed *t* test, $p < 0.0001$ *versus* PE). *B,* γKA-PE induces IL-8 expression (*, two-tailed *t* test, $p < 0.001$ *versus* PE).

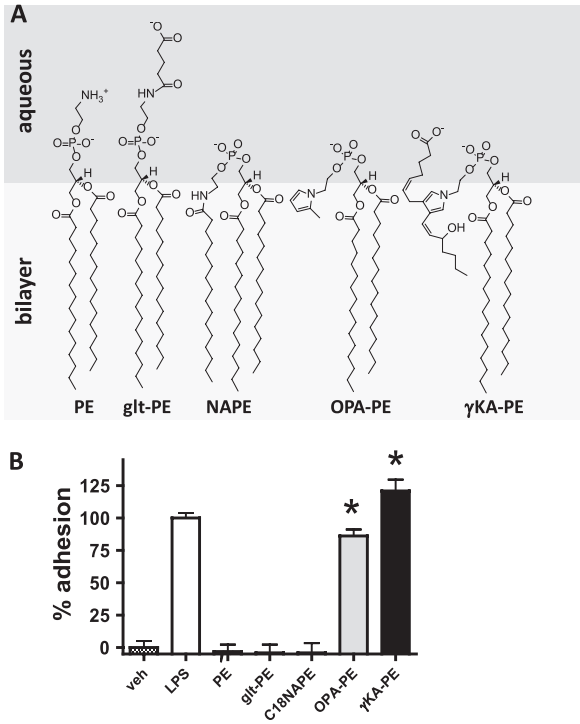

FIGURE 5. **Pyrrole moiety of γKA-PE sufficient to induce THP-1 adhesion.** *A,* potential membrane conformation of structural analogs of γKA-PE tested for the ability to induce HUVEC activation. *B,* induction of THP-1 binding to HUVEC induced by treatment with 5 μM γKA-PE or its various analogs (*, two-tailed *t* test *versus* PE, $p < 0.0001$).

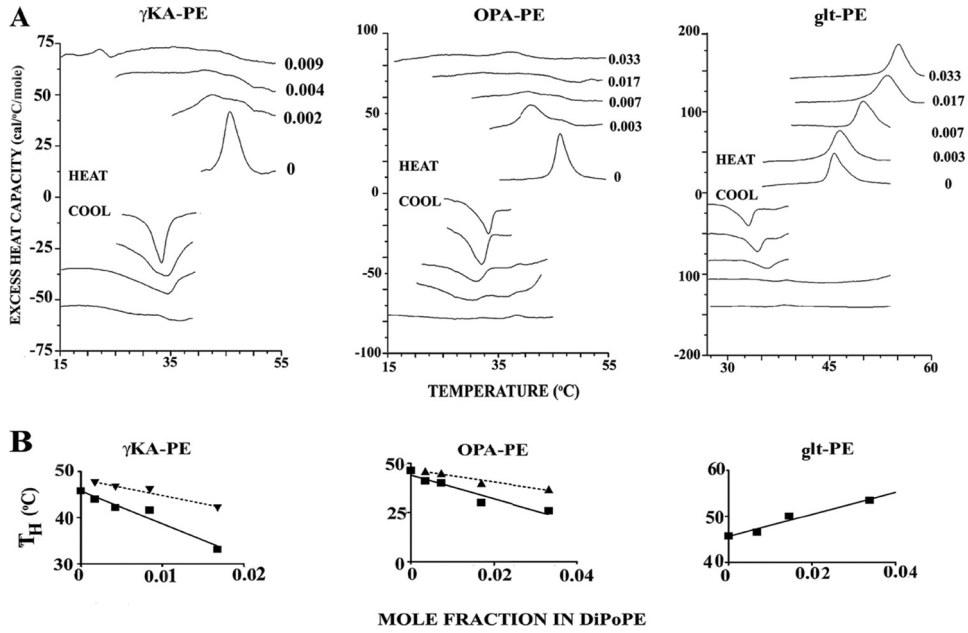

FIGURE 6. **Effect of γKA-PE and analogs on liquid crystalline to hexagonal phase transition temperature.** Differential scanning calorimetry to determine T_H of DiPoPE upon addition of incremental mole fractions of compounds was performed as described under "Experimental Procedures." *A,* representative heating and cooling differential calorimetry scans. *Left panel* corresponds to the addition of γKA-PE; *middle panel* corresponds to OPA-PE; and *right panel* corresponds to glt-PE. The *top scans* represent heating scans, and the *bottom scans* represent cooling scans. The *number* next to the heating scans gives the mole fraction of modified PE in the mixture with DiPoPE. There is a shift in temperature between heating and cooling scans because of kinetics effects. *B,* shift in T_H upon the addition of increasing mole fractions of additive. Data were taken from heating scans shown in *A*. The values of the linear regressions are shown in Table 1. The *solid line*, with ■, corresponds to the main peak of the transition, and the *dotted line*, with ▼, corresponds to a second peak appearing as a result of a split in the main transition peak.

PE Modified with Pyrrole Moieties Alters Membrane Bilayers—Membrane structure has a critical impact on cell function and membrane protein activities. One important property of both biological and model membranes is membrane curvature (27, 28), which has been shown to be important for the functioning of the endoplasmic reticulum (28–31). We hypothesized that modification of PE by pyrrole-forming aldehydes would significantly alter intrinsic membrane monolayer curvature as the pyrrole moiety seems likely to partition near the bilayer/aqueous interface, thereby disrupting normal packing and increasing the lateral pressure at some depth in the membrane (Fig. 5*A*). A consequence of such lateral pressure would be to increase the negative curvature of the monolayer in which these modified PEs are inserted. A simple and convenient measure of curvature tendency is to determine shifts in the bilayer to T_H of a model membrane composed of DiPoPE. We therefore investigated the effect of γKA-PE and its analogs on the T_H of DiPoPE using differential scanning calorimetry (Fig. 6*A*). For each set of differential scanning calorimetry curves generated, T_H was plotted against the mole fraction of modified PE. A representative plot from a one set of differential scanning calorimetry curves for each modified PE is shown in Fig. 6*B*. T_H varied slightly when measured over a longer period of time or with different batches of the same lipid. All measurements were repeated at least twice, and the calculated temperature shifts and deviations are summarized in Table 1.

γKA-PE and OPA-PE showed similar behavior, with increasing concentrations of these compounds resulting in a significant broadening of the transition and a lowering of the transition temperature for formation of T_H. This is shown in both heating and cooling curves. Such changes are consistent with these pyrrole-containing PEs increasing negative membrane curvature. In contrast, glt-PE did not broaden the transition and significantly increased the T_H, consistent with it having opposite effects and promoting positive curvature.

TABLE 1
Shifts in T_H of DiPoPE with the addition of other lipids

Additive	Shift in T_H
	degrees/mol fraction
γKA-PE	−710 ± 90
OPA-PE	−600 ± 110
glt-PE	+480 ± 70

γKA-PE Localizes to the Endoplasmic Reticulum—Various lipid mediators have been shown to exert their effects by various mechanisms, including through G-protein-coupled receptors at the plasma membrane, nuclear receptors in the nucleus, stress signaling kinases in the cytoplasm, and stress response receptors in the mitochondria and the endoplasmic reticulum. To gain insight into the cellular compartment where γKA-PE activated signaling, we synthesized a fluorescently labeled γKA-PE analog, γKA-NBD-PE. We then incubated HUVEC with γKA-NBD-PE at 4 °C for 1 h to load the plasma membrane and then initiated intracellular trafficking by raising the incubation temperature to 37 °C. After 15 min, the cells were fixed, and the localization of γKA-NBD-PE was visualized by fluorescence microscopy. When extracts of replicate-treated HUVEC were analyzed by thin layer chromatography, the major NBD-labeled compound migrated similarly to the starting γKA-NBD-PE, indicating that intracellular fluorescence represented largely intact γKA-NBD-PE (data not shown). Fluorescence imaging revealed that γKA-NBD-PE was quickly trafficked to the perinuclear region characteristic of endoplasmic reticulum

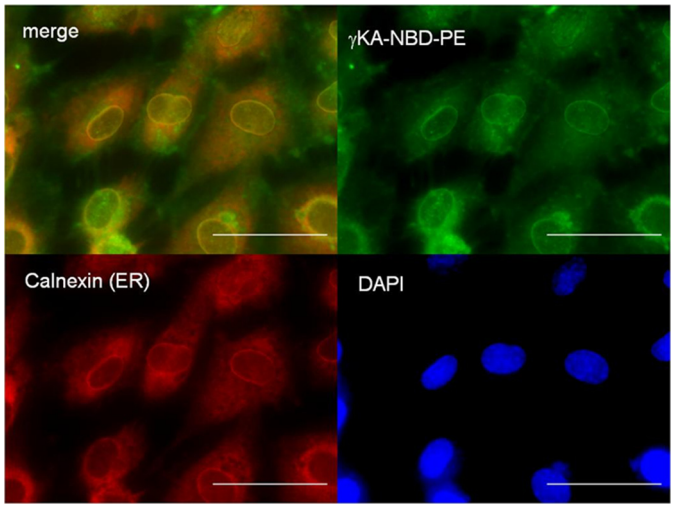

FIGURE 7. **γKA-PE localizes to endoplasmic reticulum.** Fluorescently labeled γKA-PE (γKA-NBD-PE, 1 μM) was incubated with HUVEC for 1 h at 4 °C and then for 15 min at 37 °C. HUVEC were fixed and immunostained with anti-calnexin antibodies to identify the endoplasmic reticulum and with DAPI to identify nuclei. *Upper left panel* is merged fluorescence image of γKA-NBD-PE (*green, upper right panel*) and anti-calnexin staining (*red, lower left panel*). *Yellow* color indicates colocalization of the γKA-NBD-PE and ER membrane. *Lower right panel* is nuclear (DAPI) staining of the cells. The *scale bar,* 5 μm.

(Fig. 7). Immunochemical staining of calnexin, an ER membrane marker, demonstrated significant co-localization of γKA-NBD-PE and calnexin, consistent with γKA-NBD-PE localization to ER membranes.

γKA-PE Initiates ER Stress Response Signaling—The localization of γKA-PE to the ER and the marked membrane disrupting effects of γKA-PE suggested to us the possibility that γKA-PE might invoke HUVEC activation via ER stress signaling. ER stress is sensed by the following three transmembrane proteins in the ER: PERK, IRE1, and ATF6. These three proteins result in the coordinate expression of a host of responses, including increased expression of CHOP and the ER chaperone protein BiP, as well as activation of the stress response kinase p38 MAPK via phosphorylation. To test whether γKA-PE induced ER stress response signaling, we treated HUVEC cells with either 3 μM PE (control) or γKA-PE for 10, 30, and 60 min and quantified the expression of CHOP, BiP, and phospho-p38 MAPK by immunoblotting (Fig. 8*A*). Treatment with γKA-PE resulted in ~3-fold higher levels of CHOP compared with PE at all three of the tested time points (Fig. 8*B*), as well increased BiP expression (Fig. 8*C*) and phospho-p38 MAPK (Fig. 8*D*). Increased rate of phosphorylation, rather than increased expression of p38 MAPK appeared to underlie the increase in phospho-p38 MAPK, as γKA-PE increased the phospho-p38 MAPK to total p38 MAPK ratio about 2-fold (data not shown). Thus, γKA-PE induces at least some representative elements of the ER stress response.

Inhibitors of ER Stress Response Modulate γKA-PE-Induced EC Activation—Because ER stress response signaling has been previously implicated in the induction of inflammatory chemokines (32, 33), we tested the effects of two chemical inhibitors of the ER stress response, TUDCA and AEBSF, on γKA-PE induced responses. TUDCA is a chemical chaperone that inhibits the ER stress response induced by a variety of effectors, including tunicamycin (34), thapsigargin (35), and free fatty acids (36). AEBSF is a broad spectrum serine protease inhibitor that prevents site 1 protease cleavage of ATF6, a required step in the activation of the ATF6 arm of the ER stress response (37). Preincubation for 1 h with either AEBSF (300 μM) or TUDCA (300 μM) inhibited the expression of CHOP (Fig. 9*A*) or BiP (Fig. 9*B*) induced by 3 μM γKA-PE. We then tested the effects of inhibiting this ER stress response signaling on the ability of γKA-PE to induce THP-1 adhesion to HUVEC. AEBSF inhibited THP-1 adhesion induced in response to HUVEC stimulation with 2 and 5 μM γKA-PE by 57 and 33%, respectively (Fig. 9*C*). TUDCA inhibited THP-1 adhesion in response to 2 and 5 μM γKA-PE by 78 and 64%, respectively (Fig. 9*D*). Therefore, inhibiting the ER stress response signaling by two unrelated mechanisms both leads to significantly lower induction of inflammatory responses by γKA-PE, suggesting that γKA-PE induces its effect at least in part by inducing ER stress.

DISCUSSION

The biological effects of reactive lipid aldehydes have generally been thought to result from protein and DNA modification. Our results demonstrate that PE modification is also biologically important because PE modified by γKA activates the proinflammatory response of endothelial cells. Furthermore, modification of PE may be the primary mechanism whereby γKA induces its inflammatory effect on these cells, because γKA-PE was at least as potent as γKA itself, and we had previously found that modified PE is the major product in γKA-treated endothelial cells (17). Because oxidative stress increases plasma levels of γKA-PE (18), our results suggest the possibility that the oxidative stress associated with the early stages of atherosclerosis generates γKA-PE that then contributes to the activation of endothelial cells and atherogenesis.

Whether sufficient levels of γKA-PE or other pyrrole-PEs are generated in the vascular wall during the early stages of atherosclerosis to induce inflammatory effects remains to be determined. Although relatively high concentrations of γKA-PE (1–3 μM) were required to activate inflammatory responses in our cultured HUVEC, only ~10% of γKA-PE incorporated into the cells during the assay. This is important to keep in mind as the mole fraction of γKA-PE in the membrane may be more relevant than the concentration in solution. When γKA-PE is generated endogenously, almost all of it would be expected to remain in the membrane due to its poor solubility in water. The concentration of γKA-PE found in whole livers of mice chronically fed ethanol was found to be ~30 nM (18). These levels of γKA-PE may be sufficient to induce inflammation, especially if the formation of γKA-PE in these livers is localized to the membrane of vascular cells rather than homogeneously diffuse. Our findings provide a clear rationale for future studies to directly determine the levels of γKA-PE generated in vascular membranes during early atherogenesis and other inflammatory conditions.

Our results demonstrate that γKA-PE differed from the previously described class of proinflammatory phospholipids, the CD36-binding oxPCs (38, 39). Unlike oxPCs, where the lipid whisker moiety confers activity (40), the *N*-pyrrole moiety of γKA-PE appears to be sufficient to confer activity because OPA-PE, which lacks any lipid-whisker moiety, was also active.

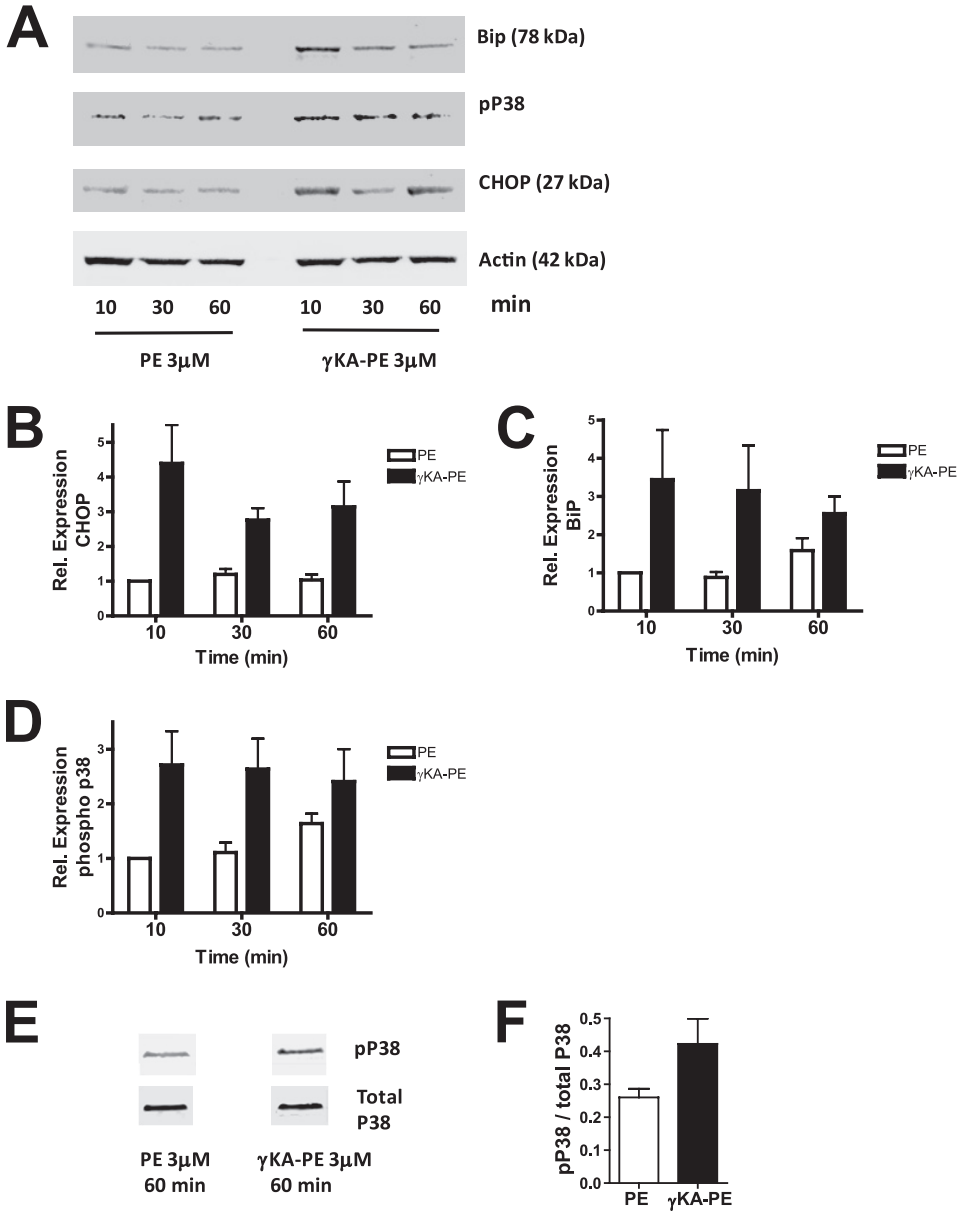

FIGURE 8. **γKA-PE induces elements of the ER stress response.** HUVEC were treated with 3 μM PE or γKA-PE for 10–60 min, lysates generated, and induction of three representative elements of the ER stress response measured by immunoblotting as described under "Experimental Procedures." *A,* immunoblots for BiP/grp78, phospho-p38, CHOP, and actin from a representative experiment. Actin was used as an internal loading control for each sample. *B,* quantitation of three replicate CHOP immunoblotting experiments. For each replicate, sample was normalized to the 10-min PE treatment to determine fold increase in expression. *C,* quantitation of three replicate BiP immunoblotting experiments. *D,* quantitation of three replicate phospho-p38 experiments. *E,* immunoblot for phospho-p38 and total p38 after 60 min of incubation with 3 μM PE or γKA-PE in additional experiments to determine whether increased phospho-p38 expression resulted from increased total p38 expression or increased phosphorylation. Samples were in nonadjacent wells on same membrane. *F,* quantitation of duplicate phospho-p38 and total p38 immunoblotting experiments.

This result raises the possibility that other pyrrole-modified PEs will also initiate endothelial activation and inflammation. Lipid peroxidation generates several other aldehydes besides γKAs that form pyrrole adducts, which include oxoalkenals (*e.g.* 4-oxo-nonenal (41)), hydroxyalkenals (*e.g.* 4-hydroxynonenal (42)), and epoxyalkenals (*e.g.* 4,5-epoxydecenal (43)). Important in this regard is the previous finding that the *in vitro* oxidation of HDL, which converts HDL from an anti-inflammatory particle to a proinflammatory one, also generates large amounts of pyrrole-PEs (20). In addition to lipid peroxidation, oxidative degradation of glucose also forms pyrrole adducts (44), and levels of glycated PE increase during diabetes (45). Thus, several different pathways are likely to yield pyrrole PEs, and our findings suggest that such pyrrole PEs could potentially be a new class of proinflammatory phospholipids.

Although both γKA-PE and oxPCs induce inflammatory responses, the effect of γKA-PE on membrane intrinsic curvature is opposite that for oxPCs. Bioactive oxPCs have a polar *sn*-2 acyl chain that appears to protrude from the bilayer to form a lipid whisker (40). The absence of this oxidized acyl chain in the bilayer should reduce the lateral pressure in the nonpolar region of the membrane and thereby increase positive membrane curvature (*i.e.* convex shape). Consistent with this expected effect, addition of oxPCs to PE bilayers increases T_H

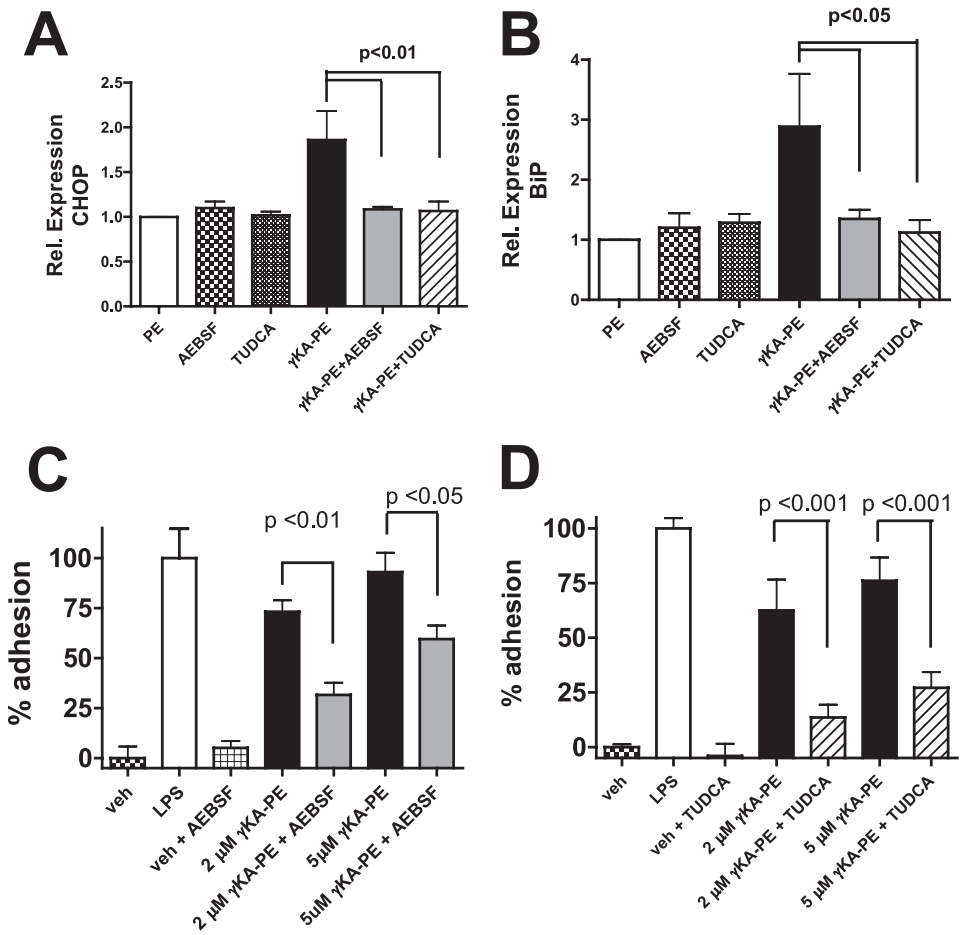

FIGURE 9. **Inhibitors of ER stress response block γKA-PE induced responses.** HUVEC were pretreated for 1 h with vehicle, 300 μM TUDCA, or 300 μM AEBSF to inhibit ER stress signaling. HUVEC were then were treated with γKA-PE for either 1 h to examine the effect on ER stress response or for 4 h to examine the effect on THP-1 adhesion. *A,* effects of pretreatment with TUDCA or AEBSF on γKA-PE (3 μM)-induced CHOP expression measured by immunoblotting. *B,* effects of pretreatment with TUDCA or AEBSF on γKA-PE (3 μM)-induced BiP expression measured by immunoblotting. *C,* effects of pretreatment with AEBSF on THP-1 induced by 2 or 5 μM γKA-PE. *D,* effects of pretreatment with TUDCA on THP-1 adhesion to HUVEC induced by 2 or 5 μM γKA-PE.

(46). In this study, we found that glt-PE, which should also form lipid whiskers, increased T_H as well. In contrast, the two pyrrole-PEs markedly reduced T_H and would therefore be expected to confer negative curvature (*i.e.* concave shape.)

Although oxPCs and pyrrole PEs have opposing effects on intrinsic membrane curvature, these opposing effects may be complementary in terms of overall physical curvature of the membrane because the major fraction of PC and PE reside on opposite monolayers of the membrane bilayer in cells. Thus, modification of PC and PE on these opposite monolayers, with their inverse effects on each monolayer, would cooperate to curve the membrane in the same direction. Such opposite, but cooperative, curvature of each monolayer has been demonstrated for the formation of membrane pores during membrane fusion promoted by viral fusion proteins (47).

Our finding that γKA-PE can invoke both ER stress signaling and inflammatory cytokines and that chemical inhibitors of the ER stress response reduce the extent to which γKA-PE activates inflammatory responses is consistent with a developing paradigm linking oxidized lipids, ER stress, inflammation, and atherosclerosis. ER stress response proteins are markedly increased in atherosclerotic lesions (48). Treatment of human endothelial cells with oxidized LDL induces all three of the transmembrane sensors for ER stress, including phosphorylation of PERK and IRE1 and ATF6 nuclear translocation (49). OxPC induces mRNA for *ATF4* and the spliced (active) version of *XBP1*, which are important downstream mediators of ER stress signaling (50), and silencing these two genes dramatically reduces oxPC induced *IL-8* and *MCP-1* expression (32). Treatment of human endothelial cells with acrolein and HNE also induces ER stress as indicated by spliced XBP-1, ATF4 nuclear localization, and increased levels of CHOP mRNA (33, 51). Furthermore, inhibition of ER stress blocks acrolein-induced increases in mRNA levels of the proinflammatory cytokines TNFα, IL-6, and IL-8 (33). As γKA, HNE, and acrolein all modify PE (8, 11, 13, 15–18), our finding that γKA-PE induces CHOP, IL-8, and MCP-1 expression raises the possibility that these other aldehydes also mediate their inflammatory effects by forming modified PE, which induce ER stress responses.

One key question that remains unanswered is the exact mechanism whereby oxidatively modified phospholipids activate ER stress signaling. Our studies suggest that γKA-PE formed at the plasma membrane will rapidly translocate to the ER and potentially alter ER curvature. One caveat in interpreting our localization study is that the presence of an NBD label on γKA-NBD-PE might have caused it to partition somewhat

differently than endogenously formed native γKA-PE. Thus, future studies will be needed to confirm that cells undergoing endogenous lipid peroxidation do in fact accumulate γKA-PE in their ER. Although ER stress is generally thought of in terms of the accumulation of unfolded proteins during protein synthesis, the ER is also the site of phospholipid and cholesterol synthesis. Overloading cells with free cholesterol or free fatty acid can induce ER stress responses (36, 52, 53). Therefore, it seems plausible that ER stress response signals might be triggered by the accumulation of the modified version of any ER product and not simply unfolded proteins. Future studies are needed to test whether γKA-PE does indeed alter ER membrane curvature and whether such alteration lead to conformational changes in and the activation of PERK, IRE1, and ATF6.

Acknowledgment—We thank Summer Young for valuable technical advice.

REFERENCES

1. Go, Y. M., Halvey, P. J., Hansen, J. M., Reed, M., Pohl, J., and Jones, D. P. (2007) *Am. J. Pathol.* **171,** 1670–1681
2. Shanmugam, N., Figarola, J. L., Li, Y., Swiderski, P. M., Rahbar, S., and Natarajan, R. (2008) *Diabetes* **57,** 879–888
3. Yamawaki, H., Saito, K., Okada, M., and Hara, Y. (2008) *Am. J. Physiol. Cell Physiol.* **295,** C1510–C1517
4. Nitti, M., Domenicotti, C., d'Abramo, C., Assereto, S., Cottalasso, D., Melloni, E., Poli, G., Biasi, F., Marinari, U. M., and Pronzato, M. A. (2002) *Biochem. Biophys. Res. Commun.* **294,** 547–552
5. Hill, G. E., Miller, J. A., Baxter, B. T., Klassen, L. W., Duryee, M. J., Tuma, D. J., and Thiele, G. M. (1998) *Atherosclerosis* **141,** 107–116
6. Lee, J. Y., Je, J. H., Kim, D. H., Chung, S. W., Zou, Y., Kim, N. D., Ae Yoo, M., Suck Baik, H., Yu, B. P., and Chung, H. Y. (2004) *Eur. J. Biochem.* **271,** 1339–1347
7. Moretto, N., Facchinetti, F., Southworth, T., Civelli, M., Singh, D., and Patacchini, R. (2009) *Am. J. Physiol. Lung Cell Mol. Physiol.* **296,** L839–L848
8. Zemski Berry, K. A., and Murphy, R. C. (2007) *Chem. Res. Toxicol.* **20,** 1342–1351
9. Balasubramanian, K., Bevers, E. M., Willems, G. M., and Schroit, A. J. (2001) *Biochemistry* **40,** 8672–8676
10. Bhuyan, K. C., Master, R. W., Coles, R. S., and Bhuyan, D. K. (1986) *Mech. Ageing Dev.* **34,** 289–296
11. Guichardant, M., Taibi-Tronche, P., Fay, L. B., and Lagarde, M. (1998) *Free Radic. Biol. Med.* **25,** 1049–1056
12. Guichardant, M., Bernoud-Hubac, N., Chantegrel, B., Deshayes, C., and Lagarde, M. (2002) *Prostaglandins Leukot. Essent. Fatty Acids* **67,** 147–149
13. Bacot, S., Bernoud-Hubac, N., Baddas, N., Chantegrel, B., Deshayes, C., Doutheau, A., Lagarde, M., and Guichardant, M. (2003) *J. Lipid Res.* **44,** 917–926
14. Stadelmann-Ingrand, S., Pontcharraud, R., and Fauconneau, B. (2004) *Chem. Phys. Lipids* **131,** 93–105
15. Bacot, S., Bernoud-Hubac, N., Chantegrel, B., Deshayes, C., Doutheau, A., Ponsin, G., Lagarde, M., and Guichardant, M. (2007) *J. Lipid Res.* **48,** 816–825
16. Bernoud-Hubac, N., Fay, L. B., Armarnath, V., Guichardant, M., Bacot, S., Davies, S. S., Roberts, L. J., 2nd, and Lagarde, M. (2004) *Free Radic. Biol. Med.* **37,** 1604–1611
17. Sullivan, C. B., Matafonova, E., Roberts, L. J., 2nd, Amarnath, V., and Davies, S. S. (2010) *J. Lipid Res.* **51,** 999–1009
18. Li, W., Laird, J. M., Lu, L., Roychowdhury, S., Nagy, L. E., Zhou, R., Crabb, J. W., and Salomon, R. G. (2009) *Free Radic. Biol. Med.* **47,** 1539–1552
19. Bach, D., Epand, R. F., Epand, R. M., Miller, I. R., and Wachtel, E. (2009) *Chem. Phys. Lipids* **161,** 95–102
20. Hidalgo, F. J., Nogales, F., and Zamora, R. (2004) *Anal. Biochem.* **334,** 155–163
21. Guo, L., Amarnath, V., and Davies, S. S. (2010) *Anal. Biochem.* **405,** 236–245
22. Amarnath, V., Amarnath, K., Matherson, T., Davies, S., and Roberts, L. J. (2005) *Synthetic Commun.* **35,** 397–408
23. Amarnath, V., Amarnath, K., Amarnath, K., Davies, S., and Roberts, L. J., 2nd. (2004) *Chem. Res. Toxicol.* **17,** 410–415
24. Kilgore, K. S., Shen, J. P., Miller, B. F., Ward, P. A., and Warren, J. S. (1995) *J. Immunol.* **155,** 1434–1441
25. Epand, R. M. (1985) *Biochemistry* **24,** 7092–7095
26. Privalov, G., Kavina, V., Freire, E., and Privalov, P. L. (1995) *Anal. Biochem.* **232,** 79–85
27. Graham, T. R., and Kozlov, M. M. (2010) *Curr. Opin. Cell Biol.* **22,** 430–436
28. Shibata, Y., Hu, J., Kozlov, M. M., and Rapoport, T. A. (2009) *Annu. Rev. Cell Dev. Biol.* **25,** 329–354
29. Friedman, J. R., Webster, B. M., Mastronarde, D. N., Verhey, K. J., and Voeltz, G. K. (2010) *J. Cell Biol.* **190,** 363–375
30. Park, S. H., and Blackstone, C. (2010) *EMBO Rep.* **11,** 515–521
31. Settles, E. I., Loftus, A. F., McKeown, A. N., and Parthasarathy, R. (2010) *Biophys. J.* **99,** 1539–1545
32. Gargalovic, P. S., Gharavi, N. M., Clark, M. J., Pagnon, J., Yang, W. P., He, A., Truong, A., Baruch-Oren, T., Berliner, J. A., Kirchgessner, T. G., and Lusis, A. J. (2006) *Arterioscler. Thromb. Vasc. Biol.* **26,** 2490–2496
33. Haberzettl, P., Vladykovskaya, E., Srivastava, S., and Bhatnagar, A. (2009) *Toxicol. Appl. Pharmacol.* **234,** 14–24
34. Ozcan, U., Yilmaz, E., Ozcan, L., Furuhashi, M., Vaillancourt, E., Smith, R. O., Görgün, C. Z., and Hotamisligil, G. S. (2006) *Science* **313,** 1137–1140
35. Lee, Y. Y., Hong, S. H., Lee, Y. J., Chung, S. S., Jung, H. S., Park, S. G., and Park, K. S. (2010) *Biochem. Biophys. Res. Commun.* **397,** 735–739
36. Jiao, P., Ma, J., Feng, B., Zhang, H., Alan Diehl, J., Eugene Chin, Y., Yan, W., and Xu, H. (2011) *Obesity* ***19,*** 483–491
37. Okada, T., Haze, K., Nadanaka, S., Yoshida, H., Seidah, N. G., Hirano, Y., Sato, R., Negishi, M., and Mori, K. (2003) *J. Biol. Chem.* **278,** 31024–31032
38. Podrez, E. A., Poliakov, E., Shen, Z., Zhang, R., Deng, Y., Sun, M., Finton, P. J., Shan, L., Gugiu, B., Fox, P. L., Hoff, H. F., Salomon, R. G., and Hazen, S. L. (2002) *J. Biol. Chem.* **277,** 38503–38516
39. Podrez, E. A., Poliakov, E., Shen, Z., Zhang, R., Deng, Y., Sun, M., Finton, P. J., Shan, L., Febbraio, M., Hajjar, D. P., Silverstein, R. L., Hoff, H. F., Salomon, R. G., and Hazen, S. L. (2002) *J. Biol. Chem.* **277,** 38517–38523
40. Greenberg, M. E., Li, X. M., Gugiu, B. G., Gu, X., Qin, J., Salomon, R. G., and Hazen, S. L. (2008) *J. Biol. Chem.* **283,** 2385–2396
41. Zhang, W. H., Liu, J., Xu, G., Yuan, Q., and Sayre, L. M. (2003) *Chem. Res. Toxicol.* **16,** 512–523
42. Sayre, L. M., Arora, P. K., Iyer, R. S., and Salomon, R. G. (1993) *Chem. Res. Toxicol.* **6,** 19–22
43. Hidalgo, F. J., Nogales, F., and Zamora, R. (2008) *Food Chem. Toxicol.* **46,** 43–48
44. Njoroge, F. G., Sayre, L. M., and Monnier, V. M. (1987) *Carbohydr. Res.* **167,** 211–220
45. Miyazawa, T., Nakagawa, K., Shimasaki, S., and Nagai, R. (2010) *Amino Acids,* doi: 10.1007/s00726-010-0772-3
46. Epand, R. F., Mishra, V. K., Palgunachari, M. N., Anantharamaiah, G. M., and Epand, R. M. (2009) *Biochim. Biophys. Acta* **1788,** 1967–1975
47. Razinkov, V. I., Melikyan, G. B., Epand, R. M., Epand, R. F., and Cohen, F. S. (1998) *J. Gen. Physiol.* **112,** 409–422
48. Tabas, I. (2009) *Antioxid. Redox. Signal.* **11,** 2333–2339
49. Sanson, M., Augé, N., Vindis, C., Muller, C., Bando, Y., Thiers, J. C., Marachet, M. A., Zarkovic, K., Sawa, Y., Salvayre, R., and Nègre-Salvayre, A. (2009) *Circ. Res.* **104,** 328–336
50. Gargalovic, P. S., Imura, M., Zhang, B., Gharavi, N. M., Clark, M. J., Pagnon, J., Yang, W. P., He, A., Truong, A., Patel, S., Nelson, S. F., Horvath, S., Berliner, J. A., Kirchgessner, T. G., and Lusis, A. J. (2006) *Proc. Natl. Acad. Sci.* **103,** 12741–12746
51. West, J. D., and Marnett, L. J. (2005) *Chem. Res. Toxicol.* **18,** 1642–1653
52. Devries-Seimon, T., Li, Y., Yao, P. M., Stone, E., Wang, Y., Davis, R. J., Flavell, R., and Tabas, I. (2005) *J. Cell Biol.* **171,** 61–73
53. Karaskov, E., Scott, C., Zhang, L., Teodoro, T., Ravazzola, M., and Volchuk, A. (2006) *Endocrinology* **147,** 3398–3407